AIMS Materials Science, 10(1): 70–85.
DOI: 10.3934/matersci.2023005
Received: 08 July 2022
Revised: 29 November 2022
Accepted: 22 December 2022
Published: 10 January 2023

http://www.aimspress.com/journal/Materials

Case report

Increasing the charge/discharge rate for phase-change materials by forming hybrid composite paraffin/ash for an effective thermal energy storage system

Budhi Muliawan Suyitno*, Dwi Rahmalina and Reza Abdu Rahman

Department of Mechanical Engineering, Faculty of Engineering, Universitas Pancasila, Srengseng Sawah, Jagakarsa 12640, DKI Jakarta, Indonesia

* **Correspondence:** Email: budhi.suyitno@univpancasila.ac.id.

Abstract: Low-temperature latent heat storage (LHS) systems are suitable for incorporating paraffin as the storage material. However, they face difficulty in actual implementation due to low thermal conductivity (TC). The present study used volcanic ash as an environmentally friendly and cost-effective material to increase the TC of paraffin. Three composites of paraffin/ash were prepared with ash proportions of 10 wt%, 30 wt% and 50 wt%. Characterizations were done to evaluate the average TC and properties. Thermal performance evaluation was conducted by analyzing the static charge/discharge cycle. The average TC for paraffin was 0.214 W/m·K. Adding volcanic ash improved the TC to 19.598 W/m·K. It made the charge/discharge performance of the composite better than that of pure paraffin. The charge rate for the composite ranged from 3.83 °C/min to 5.12 °C/min. The highest discharge rate was obtained at 4.21 °C/min for the composite $paraffin_{50}/ash_{50}$. The freezing temperature for the composite is influenced by the ash proportion, which can be taken as a suitable approach to adjust the freezing point of paraffin-based thermal energy storage (TES). The detailed results for the characterization and thermal performance evaluation are described thoroughly within the article. The overall result indicates that volcanic ash is applicable for improving the TC and charge/discharge rate of paraffin-based TES.

Keywords: ash; paraffin; phase change materials; thermal conductivity; thermal energy storage

1. Introduction

The risks of the energy crisis and global warming are motivating researchers across the globe to utilize alternative energy sources while simultaneously improving the reliability of renewable energy sources. Moreover, increasing the efficiency of the existing energy system is considered a suitable method to reduce the consumption of primary energy sources that still rely on fossil fuels [1]. Recent trends indicate that the deployment of solar and wind energy as renewable energy sources is increasing exponentially [2]. As a result, the annual global renewable energy production has increased rapidly in the last 10 years. Rapid growth in renewable energy deployment is related to the advanced development of energy storage systems, particularly for thermal energy storage (TES) [3]. TES is gaining momentum as an attractive method to store thermal energy. It can be implemented as a thermal substitution that reduces fossil fuel consumption indirectly for the heating/cooling sector. Continuous effort for optimization is still in progress, focusing on system improvement to provide more reliable and efficient thermal storage [4].

Sensible and latent heat storage are the two common methods for TES systems. Sensible heat storage utilizes the specific heat capacity of the storage material as the mechanism to store thermal energy. It is the most mature technology but suffers from low gravimetric and volumetric energy density [5]. Latent heat storage (LHS) uses a phase-change material (PCM) which stores the thermal energy based on its enthalpy of fusion. Thus, it can store sufficient thermal energy during the phase transition at a relatively small temperature gradient [6]. Furthermore, PCMs can be combined by using its specific heat capacity during the solid and liquid sensible stage, so they act as a sensible material. Therefore, the storage capacity can be improved significantly based on the specific heat capacity at a given temperature operation and its enthalpy of fusion [7]. PCMs can be applied in active and passive thermal storage systems, making them suitable for various applications, such as residential heating/cooling and solar thermal systems [8].

Paraffin wax is the ideal candidate for a PCM for a low-temperature LHS system owing to its high enthalpy of fusion (approximately 180 kJ/kg) [9]. A PCM with a high enthalpy of fusion is desirable for LHS since it provides a higher storage capacity. The enthalpy of fusion is the key indicator for determining the storage capacity of the LHS system. The theoretical phase transition occurs at a constant temperature (isothermal phase transition), which makes the system absorb and release thermal energy isothermally [10]. Furthermore, paraffin is cheap, stable at room temperature and a non-corrosive substance. Low-temperature applications such as residential water heaters and thermal management systems are suitable for paraffin-based PCMs.

Two problems are related to the actual implementation of paraffin in LHS systems. The problems are related to the unstable phase transition [11] and low thermal conductivity [12]. Polymer can be used as a supporting matrix to promote the stable phase transition of paraffin. It can also maintain the long-term performance of the LHS system for up to 5000 charge/discharge cycles [13]. The next issue is related to low thermal conductivity. During the operation, the heat exchange process requires interaction between the paraffin and thermal source/load, which is highly dependent on thermal conductivity [14]. Low thermal conductivity decreases the heat transfer coefficient during the operation. As a result, the system operates at a slow charge/discharge cycle, which reduces the overall performance of the system substantially [15].

Two approaches can be taken to overcome the low thermal conductivity issue for paraffin-based PCMs. It can be done by promoting a better heat transfer rate based on the configuration of the

storage container for paraffin-based PCMs. Yang et al. used modified fins inside the storage container. The charge rate of the finned container was 65% higher than that of the container without fins [16]. Waser et al. studied the combination of tube-in-shell and fin-based heat exchangers for the storage container [17]. It reduced the supercooling effect, which promotes a higher discharge rate. Bayomy et al. developed a storage container with a coil heat exchanger to accelerate the heat transfer process of paraffin-based TES. The proposed model increased the overall efficiency to 82% [18]. In general, using a suitable heat exchanger in the storage container minimizes the effect of low thermal conductivity. Kalapala and Devanuri confirmed that the heat transfer coefficient from the heat exchanger within the storage tank greatly influences the overall performance of an active LHS system [19].

A high thermal conductivity material can be used as an additive to develop a composite paraffin. The method is applicable for active and passive LHS systems. Deng et al. used a metal matrix to create a composite paraffin, proving that the melting/freezing processes increased by 93.9% and 95.9%, respectively [20]. Chen et al. utilized copper foams to improve the conductivity of a composite paraffin/polymer [21]. Qu et al. added 5-wt% carbon nanotubes to composite paraffin/high-density polyethylene (HDPE) and obtained an increment in the thermal conductivity of the composite of 60% [22]. Sheikholeslami et al. proposed a combined method to enhance the low thermal conductivity of paraffin-based PCMs. They used a fin-based container and composite paraffin with high thermal conductivity nanoparticles. It increased the heat transfer rate of the system substantially [23]. However, it is hard to implement the method for an integrated LHS system, particularly for a passive storage system for residential heating/cooling systems [11]. Furthermore, it leads to a significant challenge related to the mass production of paraffin-based PCMs as low-cost thermal storage material [24].

The thermal conductivity of paraffin can be improved by using a more sustainable and low-cost material such as volcanic ash. Volcanic ash is widely available, more economical, environmentally friendly and sustainable [25]. It consists of metallic and non-metallic minerals [26], which generally have better thermal conductivity than pure paraffin. It can be taken as a cost-effective material to improve the thermal conductivity in paraffin-based TES systems [27]. Considering the potential of volcanic ash to increase the thermal conductivity in paraffin-based TES systems, further characterization is required to understand the effect of volcanic ash in composite paraffin/volcanic ash. Thus, the study aimed to examine the effects of volcanic ash of different weight proportions on the thermal performance of a paraffin-based TES system. Extensive characterization was conducted to evaluate the thermal conductivity, thermal properties and stability of the composite. The micrograph observation and infrared spectrum are presented as well in the study. Moreover, static charging/discharging test was also conducted to observe the charge/discharge cycles for the composite. The findings from the study are expected to be used as an essential reference for the further development of high thermal conductivity composite paraffin/volcanic ash as a sustainable and low-cost thermal conductivity enrichment material.

2. Materials and methods

2.1. Sample preparations

Commercial-grade paraffin wax (with an average melting temperature of 60 °C) was purchased

from a local marketplace. We used volcanic ash with an average particle size of 74 μm. The main constituents of the volcanic ash were Fe (51.23%), Fe_2O_3 (23.24%) and SiO_2 (11%). The other composition and physical properties of the volcanic ash can be found in a previous report [27]. Four samples were prepared for characterization and static charging/discharging testing (Table 1). The mixing process for the composite was conducted by melting the paraffin using a thermal bath at a temperature of 90 °C. The ash was heated for 30 min in an electric oven at a temperature of 100 °C to remove the moisture. After that, the ash was added to the molten paraffin. The mixture was stirred slowly for half an hour. Then, rapid cooling was applied to the mixture to ensure that the ash dispersed properly within the solid composite. The total sample weight was 20 g for thermal evaluation through static charging/discharging testing.

2.2. Characterizations

Thermal conductivity measurement was conducted by using the hot disk method (TPS–3500). The test was repeated five times to estimate the average thermal conductivity for each sample. The enthalpy of fusion and melting and freezing temperatures were evaluated by using differential scanning calorimetry (DSC, MT + 1). The heating rate was set at 5 ℃/min to minimize the effect of thermal inertia during the heating process. The decomposition curve for each sample was assessed by using thermogravimetric analysis (TGA). Fourier-transform infrared (FTIR) spectroscopy was applied to each sample to compare the functional group between the paraffin and composites of paraffin/ash. Then, the microstructures of the paraffin and the composites were evaluated by using scanning electron microscopy (SEM).

2.3. Charge/discharge cycle

Thermal performance evaluation was conducted to examine the charge/discharge rate of the prepared samples. Figure 1 presents the schematic design for static thermal performance evaluation. Each sample was tested individually. The sample was stored within the storage container (copper tube). The charge cycle was done by heating the storage container in an oil bath with an electric heater (Figure 1a). The charge cycle for TES is an endothermic process, meaning that the storage material is heated from an external source. Oppositely, the discharge cycle is an exothermic process, meaning that the stored heat in the storage material is released to the surroundings [28].

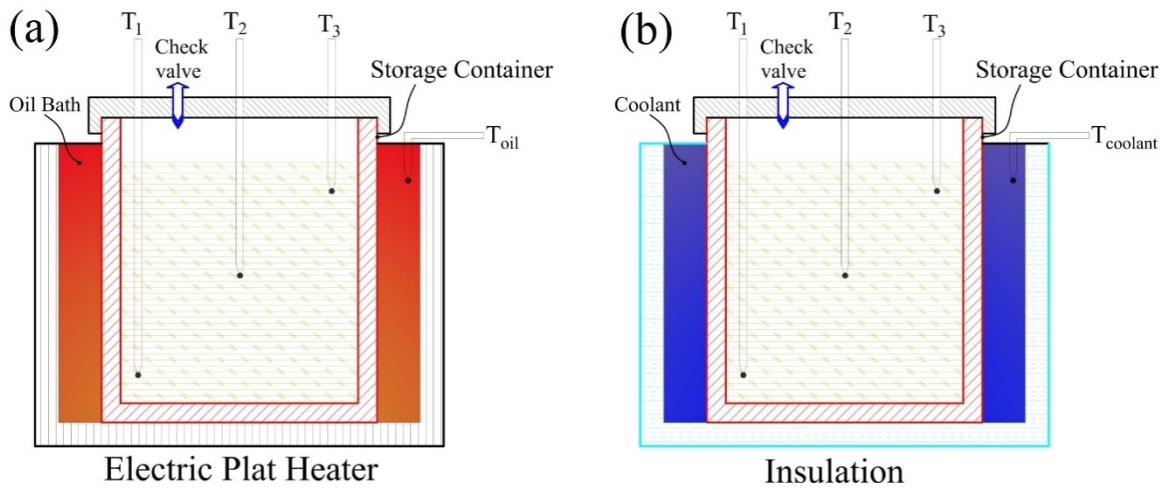

Figure 1. Schematic for charge cycle (a) and discharge cycle (b).

The composite paraffin/ash is intended for a passive LHS system. Thus, the charge cycle was limited to a temperature of 65 ℃, which is slightly higher than the melting temperature of paraffin. The charge cycle was conducted by heating the sample using an electric hot plate. Once the sample reached the target temperature (65 ℃), the storage container was moved to the cooling chamber for the discharge cycle (Figure 1b). The discharge cycle was conducted by using water as cooling media (with an initial temperature of 10 ℃). Three thermocouples (Type K) were located within the storage container to record temperature changes during the charge/discharge cycle. The result of the charge/discharge cycle has been plotted by using a temperature-time graph to analyze the charge/discharge rate for each sample [29].

3. Results

3.1. DSC results

DSC provides sufficient information about the thermal properties of the prepared samples. It shows different heating/cooling curves, indicating the effect of the ash content within the composite (Figure 2). Paraffin yielded two endothermic peaks, indicating two crystallinity behaviors during the heating process. The first peak marks the solid-solid transition, which occurred around 40 ℃. The second endothermic peak occurred at a temperature of 61.4 ℃, representing the melting temperature of paraffin with an enthalpy of fusion of 188.7 J/g.

There was no substantial change in the heating curve for the composite $paraffin_{90}/ash_{10}$. The first and second peaks of the composite were relatively similar to those of pure paraffin. It had a melting temperature of 60.9 ℃ with an enthalpy of fusion of 179.2 J/g. Contrary to that, the heating curve was changed significantly for the composites with a higher ash content. As shown in Figure 2, the endothermic peak decreased for $paraffin_{70}/ash_{30}$ and $paraffin_{50}/ash_{50}$. The melting temperatures of both samples were 60.3 ℃ and 56.4 ℃, respectively. The enthalpies of fusion of both samples were 175.6 J/g ($paraffin_{70}/ash_{30}$) and 158.5 J/g ($paraffin_{50}/ash_{50}$). The decrement in melting temperature made the sample easier to melt, which is advisable for specific applications.

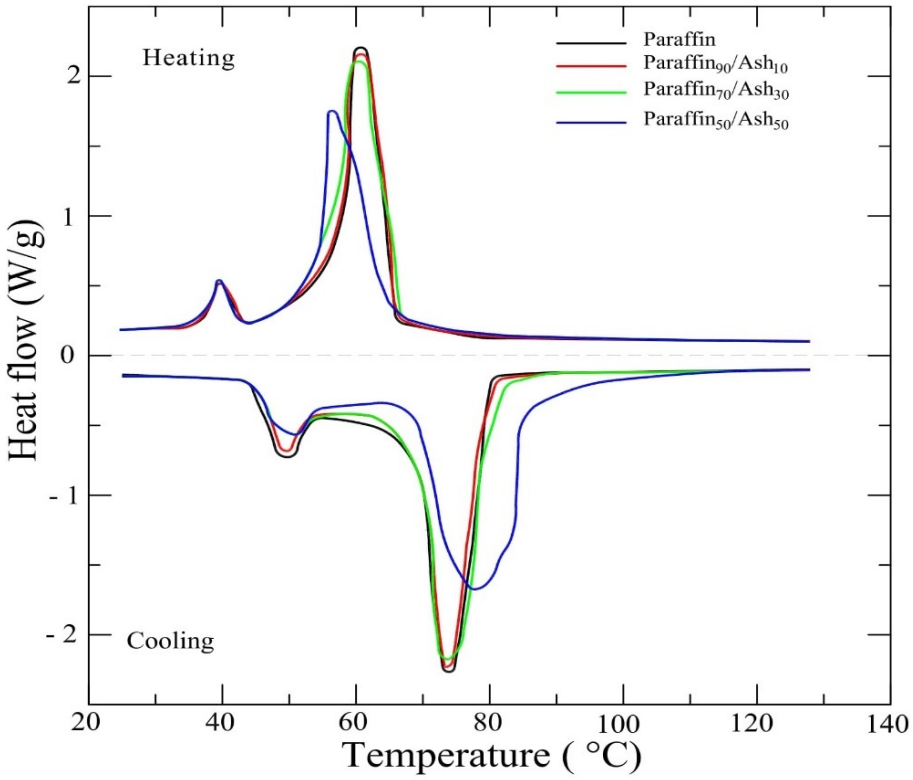

Figure 2. Heating and cooling curves for paraffin and composites of paraffin/ash.

The exothermic curve indicates the solidification process. The exothermic peak for the tested samples appeared at a higher temperature than the endothermic peak. The freezing temperature for paraffin was observed at 73.9 ℃. In contrast, the freezing temperature shifted for the composites, dependent on the ash proportion. The freezing temperature for the composite with 10 wt% ash was 73.1 ℃, which is lower than that of pure paraffin. Contrary to that, $paraffin_{90}/ash_{10}$ and $paraffin_{70}/ash_{30}$ had higher freezing temperatures of 74.2 ℃ and 78.5 ℃, respectively. A higher freezing temperature is desirable for specific applications requiring rapid solidification during the discharge cycle, while a lower freezing temperature reduces the supercooling degree, which is desirable for temperature-sensitive LHS systems. Thus, adding a suitable ash proportion can be considered to adjust the freezing temperature of paraffin to meet the requirements of the LHS system.

3.2. TGA

Figure 3 presents the TGA curve for the tested samples. The decomposition curve determines the thermal stability of the sample during the heating process. As shown in Figure 3, the decomposition behavior of pure paraffin occurred as a single step decomposition. Rapid decomposition ran continuously from temperature 180 to 400 ℃, with more than 90% of total mass loss. The thermal stability of paraffin is considerably low since it has a single-go decomposition at a relatively low temperature, which is undesirable for long-term cycles [30]. As compared to pure paraffin, the composites had different decomposition curves, implying the influence of the ash content within the sample.

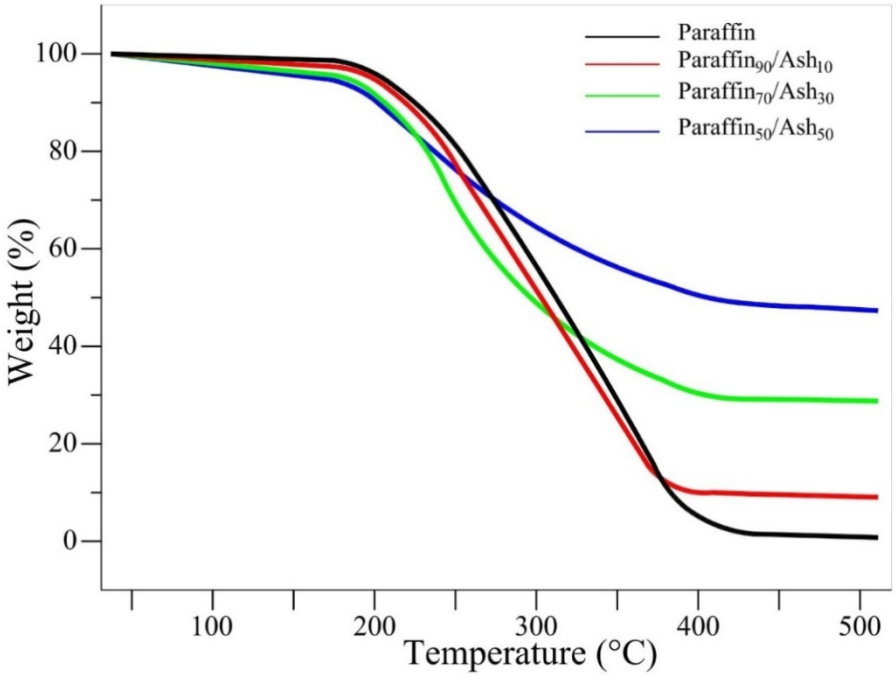

Figure 3. TGA plot for pure paraffin and composites of paraffin/ash.

The initial decomposition stage (<180 ℃) of the paraffin/ash composites revealed significant mass loss, particularly with higher ash content. It implies the decomposition of the impurities and moisture content from the ash. It suggests that the preheating treatment should be done at a higher temperature to remove the impurities and moisture within the ash. Despite that, the composites had two-stage decomposition. It implies an immiscible blend between paraffin and ash. The paraffin was decomposed in the first place until the final decomposition temperature (approximately 400 ℃) was reached. After that, no significant mass loss was observed since ash decomposes at a much higher temperature than pure paraffin.

3.3. Thermal conductivity

Figure 4 presents the average thermal conductivity of the tested samples. It shows that the thermal conductivity of paraffin is extremely low, with an average thermal conductivity of 0.214 W/m·K. It corresponds to a slow charge/discharge cycle. The average thermal conductivity of the composite paraffin/ash improved considerably. Adding 10 wt% ash increased the thermal conductivity to almost nine times that of pure paraffin. Volcanic ash is composed of various elements that generally have better thermal conductivity than paraffin. Thus, it increased the average thermal conductivity of paraffin effectively. Increasing the ash content of the composite led to a higher average thermal conductivity. However, the average thermal conductivity of the paraffin/ash composites was still much lower than the typical thermal conductivity enhancement. For instance, using copper nanoparticles increases the thermal conductivity of paraffin by up to 400 W/m·K [31].

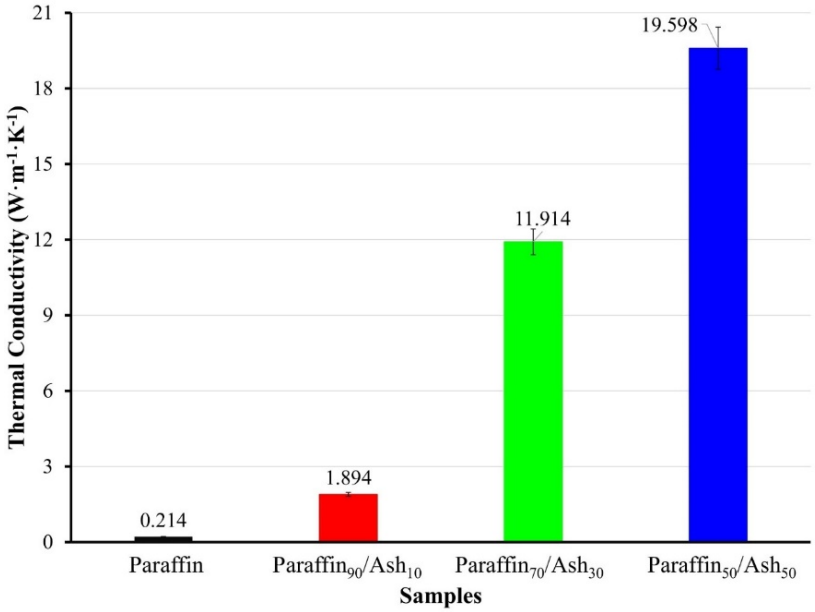

Figure 4. Average thermal conductivity of paraffin and composites of paraffin/ash.

3.4. Charge/discharge rate

The temperature-time profile for the charging stage is plotted in Figure 5. We used the average temperature from three thermocouples within the container (Figure 1). The phase transition region (indicated by the red dashed line) was accompanied by a slow temperature increment, which made the samples undergo a non-isothermal phase transition. The mushy region formation from the paraffin promoted a nonequilibrium heat transfer process. It increased the temperature slowly instead of indicating a plateau line during phase transition.

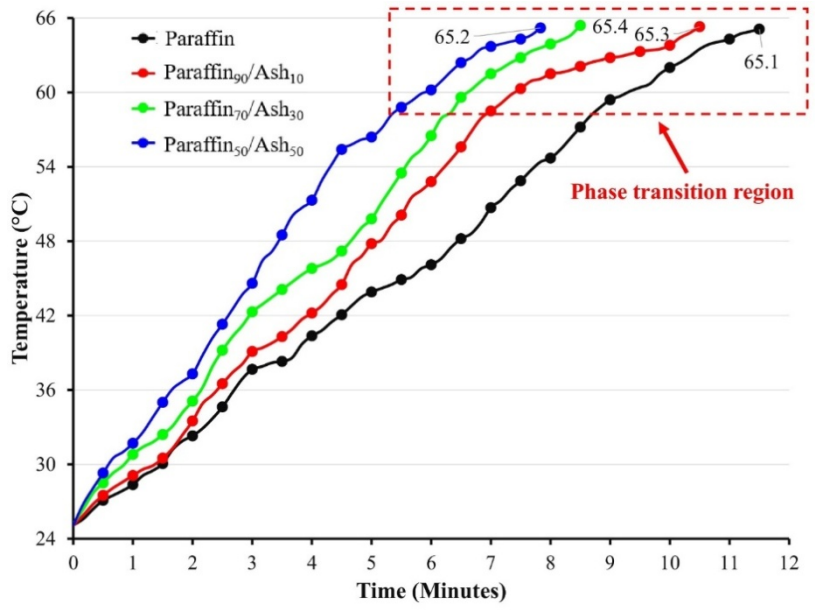

Figure 5. Temperature-time graph for charging stage for paraffin and composites of paraffin/ash.

Paraffin had the longest duration to reach the targeted temperature. Thus, it had the lowest charge rate compared to the composites of paraffin/ash. It emphasizes the effect of low thermal conductivity, which increased the duration of charge/discharge cycles during the operation. Adding ash to the paraffin directly contributed to the acceleration of the charge stage. As the thermal conductivity was enhanced, the heat transfer occurred rapidly, facilitating a better thermal distribution within the composite. Interestingly, there was a remarkable change in the temperature increment for each composite after passing the melting temperature. The temperature increment of $paraffin_{90}/ash_{10}$ was slower in the phase transition region. It implies that the effect of mushy region formation for the composite is still more noticeable than the composites with higher ash contents ($paraffin_{70}/ash_{30}$ and $paraffin_{50}/ash_{50}$). The composites $paraffin_{70}/ash_{30}$ and $paraffin_{50}/ash_{50}$ showed a steady temperature increment in the phase transition. Thus, the effect of mushy region formation can be minimized with more ash content within the composite.

The temperature increment before entering the phase transition (solid-sensible region) also accelerated distinctively. For instance, pure paraffin took 8.8 min to reach a temperature of 60 °C, while $paraffin_{90}/ash_{10}$ took a shorter duration, with only 7.3 min. A faster temperature increment in the solid-sensible region accelerated the composite to reach the phase transition region, where the most thermal energy is stored. The composite $paraffin_{50}/ash_{50}$ showed the highest charge rate, particularly during the solid-sensible stage. A higher ash content reduced the melting temperature of paraffin (Figure 2) and improved the average thermal conductivity (Figure 4). Thus, it made the charge performance of $paraffin_{50}/ash_{50}$ desirable for the operation of the LHS system.

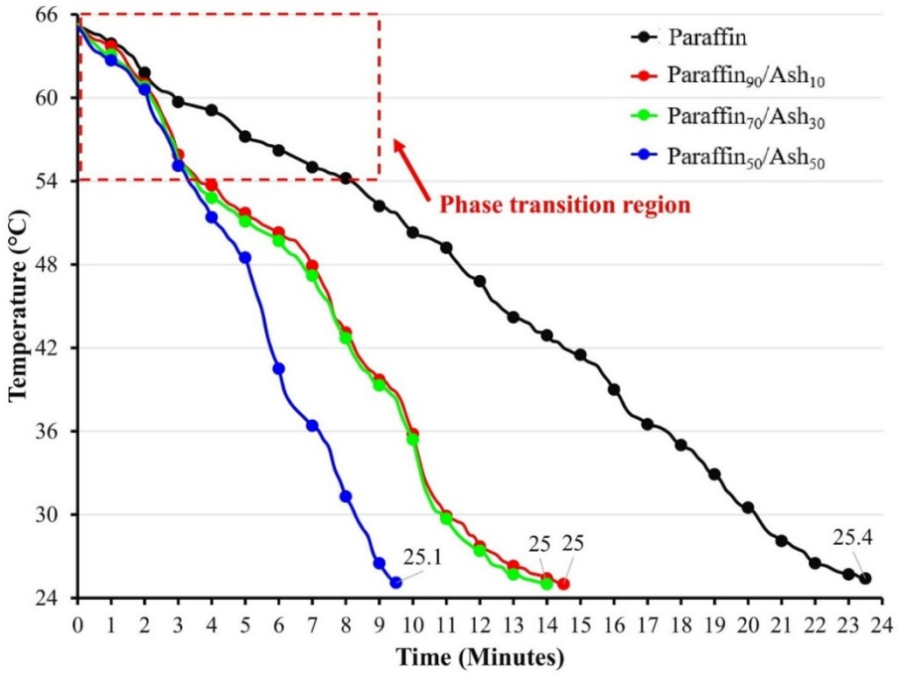

Figure 6. Temperature-time graph for discharging stage for paraffin and composites of paraffin/ash.

The discharge profile is shown in Figure 6. The heat release process for an LHS system is much slower than the charging process due to the supercooling effect [32]. Thus, the temperature decrement during the discharging process is relatively slow. For example, paraffin took almost twice

as long as the charge duration to release the stored thermal energy. It is troublesome for the actual system because it indicates a low power rate. Furthermore, mushy region formation severely affects solidification, disrupting the heat transfer process [33]. It can be observed noticeably in the phase transition region with an average temperature decrement of 1.36 °C/min. The average temperature decrement during the solid-sensible stage was slightly higher, with a discharge rate of 1.88 °C/min.

The negative impact of mushy region formation during the discharging process can be reduced by adding volcanic ash to the paraffin. It can be seen that all paraffin/ash composites had a better discharge rate in the phase transition region. The composites took approximately 4 min to reach the end stage of the solidification process. It shows the positive impact of adding volcanic ash to the paraffin, where partial phase change can be minimized. The average discharge rate for the composites with ash contents of 10 wt% and 30 wt% were 2.67 °C and 2.77 °C/min, respectively. The cooling curves for both samples (Figure 2) also show similar freezing temperatures between 73.1–74.2 °C. Therefore, the discharge characteristics for both samples were relatively similar, with sufficient heat release during the phase transition and solid-sensible stage.

Paraffin$_{50}$/ash$_{50}$ obtained the most outstanding performance since it had the highest discharge rate. The total discharge duration for paraffin$_{50}$/ash$_{50}$ was 9.5 min, which is slightly longer than the charge duration. Using a higher ash proportion promoted a better temperature distribution. Thus, the decrement during the discharge stage could be minimized. The DSC results (Figure 2) imply the same phenomenon, since paraffin$_{50}$/ash$_{50}$ had the highest deviation between melting and freezing temperatures. It corresponds to the high thermal conductivity of the composite paraffin$_{50}$/ash$_{50}$, promoting an exceptional charge/dischargeg rate.

3.5. FTIR spectra

The FTIR spectra for pure paraffin and composite paraffin/ash are plotted in Figure 7. There was no substantial change in the paraffin/ash composites relative to pure paraffin. Peak absorption mainly occurred between 2900–2800 cm^{-1}, demonstrating the stretching vibration for main functional CH_2. The next peak can be observed between 1500–1400 cm^{-1}, indicating the rocking vibration for the main functional groups $–CH_2$ and $–CH_3$. The last peak occurred around 800–700 cm^{-1}, and it is defined as rocking vibration for the main functional group of $–CH_2$. The paraffin/ash composites had spectra that were similar to that of pure paraffin. Thus, the composite was bound physically without forming any new chemical formation. Hence, the charge/discharge rate was improved by adding volcanic ash to the paraffin without altering the chemical properties of the paraffin.

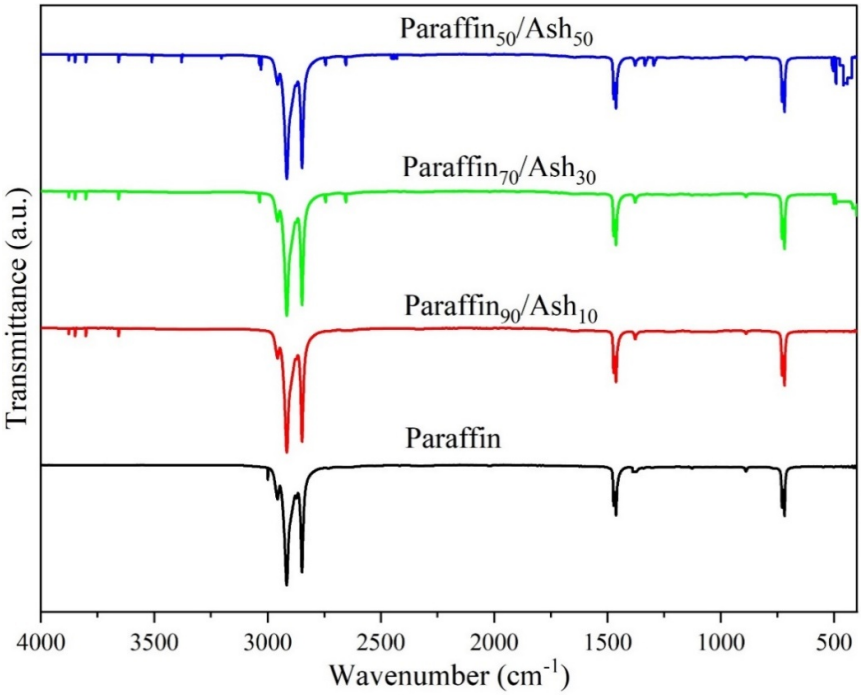

Figure 7. FTIR spectra for paraffin and composites of paraffin/ash.

3.6. SEM

Morphological observation was conducted by applying SEM to the tested samples. The SEM image was taken after thermal evaluation of the charge/discharge cycle. We intended to understand the dispersion of ash within the composite after the melting/freezing process for the actual application. Therefore, the captured images were specifically purposed to observe different morphologies which occurred within the composites of paraffin/ash. Figure 8a shows the corrugated paraffin surface affected by the melting/freezing cycle. It corresponds to the low molecular weight of paraffin and the slow freezing process, which transforms its shape after solidification. It affects the interaction between paraffin and volcanic ash, which can be seen as an immiscible blend. It confirms the TGA curve (Figure 3), which implies that the paraffin and ash melted at different rates and temperatures.

Figure 8b shows local agglomeration of the ash content within the composite. It was affected by the melting process of paraffin, which altered the ash content distribution. Since the composite $paraffin_{90}/ash_{10}$ had the lowest ash content, the solidification process caused the ash particles to agglomerate locally with the contiguous ash particles. As a result, ash agglomerated as a single cluster and formed several individual clusters (indicated by the red circle). A different ash distribution can be observed in Figure 8c. It shows that the ash dispersed moderately in the paraffin since it had a higher ash content. However, the ash particles accumulated (the green circle). The volcanic ash had a higher density than paraffin, making the particles move downward in the molten paraffin. During the freezing process, the agglomerated ash settled closely, causing local accumulation. The effect of the immiscible blend between paraffin and ash is shown in Figure 8d. It shows that a void formed around the outer layer of the ash particle (the blue circle). The void between the ash and paraffin was worsened by rapid solidification in the case of the composite

paraffin$_{50}$/ash$_{50}$ (Figure 6). It confirms the significant change in the thermal properties of the composite paraffin$_{50}$/ash$_{50}$ (Figure 2), particularly for the melting/freezing temperature; this highly corresponds to the void formation between the paraffin and ash particles.

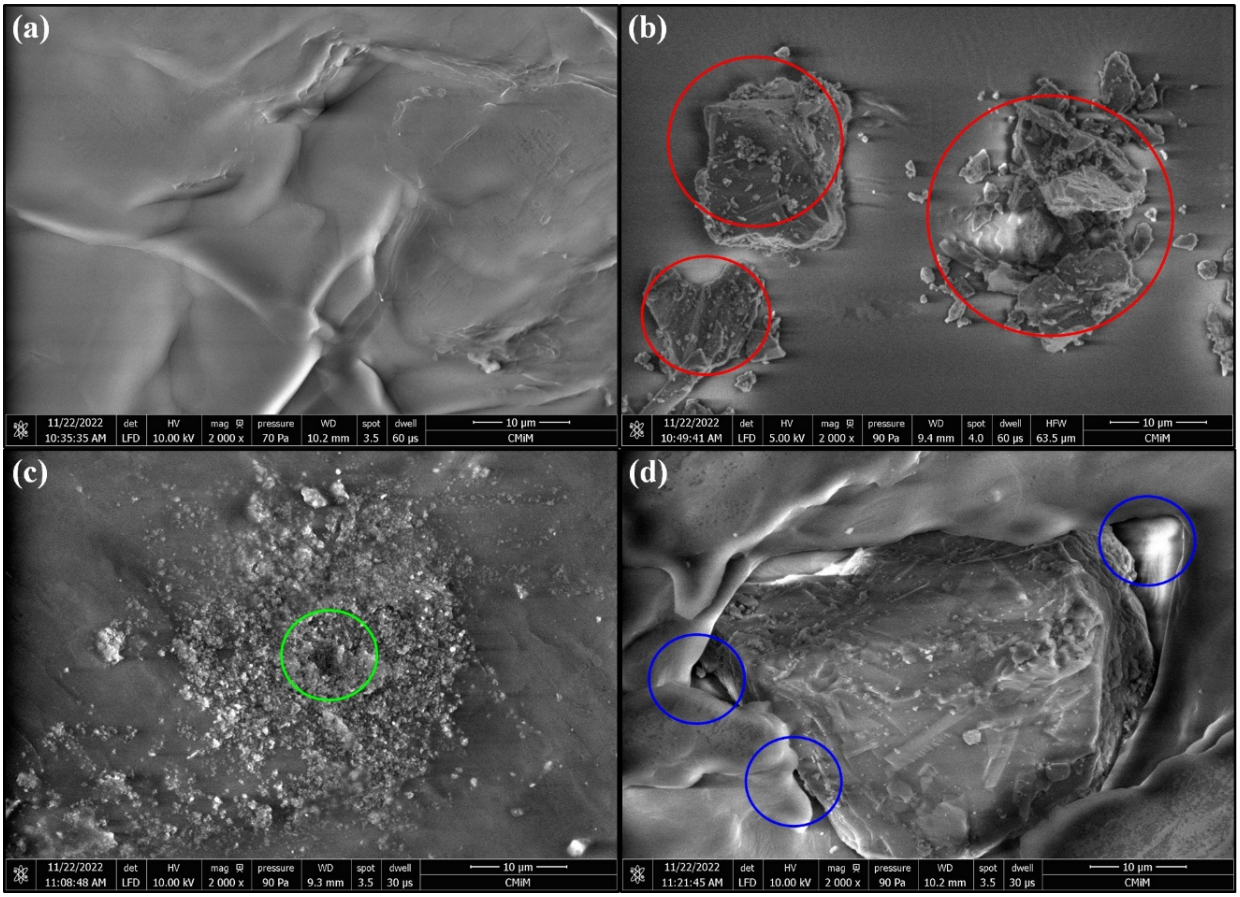

Figure 8. SEM micrographs of paraffin (a), paraffin$_{90}$/ash$_{10}$ (b), paraffin$_{70}$/ash$_{30}$ (c) and paraffin$_{50}$/ash$_{50}$ (d).

The charge/discharge rate for the paraffin/ash composite was higher than that for pure paraffin. However, sedimentation occurred for the paraffin/ash composites after 20 thermal cycles. It is an inevitable effect since volcanic ash is heavier than paraffin. The sedimentation could be minimized by using a supporting matrix such as HDPE, which works as a shape stabilizer during the phase transition of paraffin. Also, fast-charging operation causes thermal stress and hysteresis losses, potentially reducing the long-term performance of the PCM [34]. Besides its use as a shape-stabilizer, HDPE also reduces the thermal stress and hysteresis losses for fast-charging paraffin-based PCM [35]. Thus, the proposed method can be further evaluated to avoid the sedimentation and extended cycling test to evaluate the long-term operation of composites of paraffin/volcanic ash as a fast-charging LHS material.

4. Conclusion

This work examined the potential of using volcanic ash as a thermal conductivity enhancement

material for paraffin-based TES. The general results indicate that adding volcanic ash to form a paraffin/ash composite significantly improves the overall thermal conductivity. It leads to a better charge/discharge cycle. The highest discharge rate was 4.21 ℃/min, which is much higher than that for pure paraffin, with only 1.69 ℃/min. The composites of paraffin/ash had an immiscible blend that led to the FTIR spectra indicating no chemical change between the mixture. Improvement in the thermal conductivity and charge/discharge rate is correlated with the proportion of ash content within the composite. The highest thermal conductivity was 19.598 W/m·K for the composite $paraffin_{50}/ash_{50}$, which had the highest charge/discharge rate.

The addition of volcanic ash to form a composite of paraffin/ash decreased the total enthalpy of fusion. It can be considered the main drawback of adding a sensible material for thermal conductivity enhancement. The decrement in the enthalpy of fusion ranged from 5% to 16%, where the lowest decrement was obtained by $paraffin_{50}/_{50}$. Furthermore, the immiscible blend led to phase segregation and local agglomeration, which may alter the long-term performance of the composite. Despite that, improving the charge/discharge rate and thermal conductivity by adding volcanic ash can be considered as an alternative approach for increasing the performance of paraffin-based PCM. Therefore, further research is suggested to minimize the drawbacks of the volcanic ash within the composite. It can be done by using alternative binder materials such as polymers and PCMs with a higher enthalpy of fusion to maintain a suitable thermal capacity of the composite PCM and volcanic ash.

Acknowledgments

The authors would like to thanks Andika Dedi Novi Prasetyo and Adimas Aziz Tasmin for supporting the study.

Conflict of Interest

The authors declare that they have no known competing financial interests or personal relationships that could have appeared to influence the work reported in this paper.

References

1. Ismail I, Mulyanto AT, Rahman RA (2022) Development of free water knock-out tank by using internal heat exchanger for heavy crude oil. *EUREKA: Phys Eng* 77–85. https://doi.org/10.21303/2461-4262.2022.002502
2. Ismail I, Rahman RA, Haryanto G, et al. (2021) The optimal pitch distance for maximizing the power ratio for savonius turbine on inline configuration. *IJRER* 11: 595–599.
3. International Renewable Energy Agency (IRENA), Innovation outlook: Thermal energy storage, 2020. Available from: https://www.irena.org/Publications/2020/Nov/Innovation-outlook-Thermal-energy-storage.
4. Ataei A (2016) Performance optimization of a combined solar collector, geothermal heat pump and thermal seasonal storage system for heating and cooling greenhouses. *J Appl Eng Sci* 14: 296–305. https://doi.org/10.5937/jaes14-8749

5. Sadeghi G (2022) Energy storage on demand: Thermal energy storage development, materials, design, and integration challenges. *Energy Storage Mater* 46: 192-222. https://doi.org/10.1016/j.ensm.2022.01.017
6. Elbahjaoui R, El Qarnia H (2019) Performance evaluation of a solar thermal energy storage system using nanoparticle-enhanced phase change material. *Int J Hydrogen Energ* 44: 2013-2028. https://doi.org/10.1016/j.ijhydene.2018.11.116
7. Palacios A, Navarro ME, Barreneche C, et al. (2020) Hybrid 3 in 1 thermal energy storage system-Outlook for a novel storage strategy. *Appl Energ* 274: 115024. https://doi.org/10.1016/j.apenergy.2020.115024
8. Dsilva Winfred Rufuss D, Rajkumar V, Suganthi L, et al. (2019) Studies on latent heat energy storage (LHES) materials for solar desalination application-focus on material properties, prioritization, selection and future research potential. *Sol Energ Mat Sol C* 189: 149–165. https://doi.org/10.1016/j.solmat.2018.09.031
9. Yadav C, Sahoo RR (2019) Exergy and energy comparison of organic phase change materials based thermal energy storage system integrated with engine exhaust. *J Energy Storage* 24: 100773. https://doi.org/10.1016/j.est.2019.100773
10. Rahmalina D, Rahman RA, Ismail I (2022) Improving the phase transition characteristic and latent heat storage efficiency by forming polymer-based shape-stabilized PCM for active latent storage system. *Case Stud Therm Eng* 101840. https://doi.org/10.1016/j.csite.2022.101840
11. Gandhi M, Kumar A, Elangovan R, et al. (2020) A review on shape-stabilized phase change materials for latent energy storage in buildings. *Sustainability (Switzerland)* 12: 1–17. https://doi.org/10.3390/su12229481
12. Wu S, Yan T, Kuai Z, et al. (2020) Thermal conductivity enhancement on phase change materials for thermal energy storage: A review. *Energy Storage Mater* 25: 251–295. https://doi.org/10.1016/j.ensm.2019.10.010
13. Rahmalina D, Rahman RA, Ismail (2022) Increasing the rating performance of paraffin up to 5000 cycles for active latent heat storage by adding high-density polyethylene to form shape-stabilized phase change material. *J Energy Storage* 46: 103762. https://doi.org/10.1016/j.est.2021.103762
14. Ma X, Sheikholeslami M, Jafaryar M, et al. (2020) Solidification inside a clean energy storage unit utilizing phase change material with copper oxide nanoparticles. *J Cleaner Production* 245: 118888. https://doi.org/10.1016/j.jclepro.2019.118888
15. Zhang YP, Lin KP, Yang R, et al. (2006) Preparation, thermal performance and application of shape-stabilized PCM in energy efficient buildings. *Energ Buildings* 38: 1262–1269. https://doi.org/10.1016/j.enbuild.2006.02.009
16. Yang X, Lu Z, Bai Q, et al. (2017) Thermal performance of a shell-and-tube latent heat thermal energy storage unit: Role of annular fins. *Appl Energ* 202: 558–570. https://doi.org/10.1016/j.apenergy.2017.05.007
17. Waser R, Maranda S, Stamatiou A, et al. (2020) Modeling of solidification including supercooling effects in a fin-tube heat exchanger based latent heat storage. *Sol Energy* 200: 10–21. https://doi.org/10.1016/j.solener.2018.12.020
18. Bayomy A, Davies S, Saghir Z (2019) Domestic hot water storage tank utilizing phase change materials (PCMs): Numerical approach. *Energies* 12: 2170. https://doi.org/10.3390/en12112170

19. Kalapala L, Devanuri JK (2018) Influence of operational and design parameters on the performance of a PCM based heat exchanger for thermal energy storage—A review. *J Energ Storage* 20: 497–519. https://doi.org/10.1016/j.est.2018.10.024
20. Deng Z, Li J, Zhang X, et al. (2020) Melting intensification in a horizontal latent heat storage (LHS) system using a paraffin/fractal metal matrices composite. *J Energ Storage* 32: 101857. https://doi.org/10.1016/j.est.2020.101857
21. Chen P, Gao X, Wang Y, et al. (2016) Metal foam embedded in SEBS/paraffin/HDPE form-stable PCMs for thermal energy storage. *Sol Energ Mater Sol C* 149: 60–65. https://doi.org/10.1016/j.solmat.2015.12.041
22. Qu Y, Wang S, Zhou D, et al. (2020) Experimental study on thermal conductivity of paraffin-based shape-stabilized phase change material with hybrid carbon nano-additives. *Renew Energ* 146: 2637–2645. https://doi.org/10.1016/j.renene.2019.08.098
23. Sheikholeslami M, Haq R ul, Shafee A, et al. (2019) Heat transfer simulation of heat storage unit with nanoparticles and fins through a heat exchanger. *Int J Heat Mass Tran* 135: 470–478. https://doi.org/10.1016/j.ijheatmasstransfer.2019.02.003
24. Sciacovelli A, Navarro ME, Jin Y, et al. (2018) High density polyethylene (HDPE)-Graphite composite manufactured by extrusion: A novel way to fabricate phase change materials for thermal energy storage. *Particuology* 40: 131–140. https://doi.org/10.1016/j.partic.2017.11.011
25. Játiva A, Ruales E, Etxeberria M (2021) Volcanic ash as a sustainable binder material: An extensive review. *Materials* 14: 1–32. https://doi.org/10.3390/ma14051302
26. Kuznetsova E (2017) Thermal conductivity and the unfrozen water contents of volcanic ash deposits in cold climate conditions: A review. *Clays Clay Miner* 65: 168–183. https://doi.org/10.1346/CCMN.2017.064057
27. Rahmalina D, Adhitya DC, Rahman RA, et al. (2022) Improvement the performance of composite Pcm paraffin-based incorporate with volcanic ash as heat storage for low-temperature. *EUREKA-Phys Eng* 3–11. https://doi.org/10.21303/2461-4262.2022.002055
28. International Energy Agency Technology Collaboration Programme, Applications of thermal energy storage in the energy transition, 2018. Available from: https://iea-es.org/wp-content/uploads/public/86.3.3-IEA-ECES-Annex-30-Final-Report.pdf.
29. Yinping Z, Yi J (1999) A simple method, the T-history method, of determining the heat of fusion, specific heat and thermal conductivity of phase-change materials. *Meas Sci Technol* 201–205. https://doi.org/10.1088/0957-0233/10/3/015
30. Trisnadewi T, Kusrini E, Nurjaya DM, et al. (2021) Experimental analysis of natural wax as phase change material by thermal cycling test using thermoelectric system. *J Energy Storage* 40: 102703. https://doi.org/10.1016/j.est.2021.102703
31. Eanest Jebasingh B, Valan Arasu A (2020) A comprehensive review on latent heat and thermal conductivity of nanoparticle dispersed phase change material for low-temperature applications. *Energy Storage Mater* 24: 52–74. https://doi.org/10.1016/j.ensm.2019.07.031
32. Shamseddine I, Pennec F, Biwole P, et al. (2022) Supercooling of phase change materials: A review. *Renewa Sust Energ Rev* 158: 112172. https://doi.org/10.1016/j.rser.2022.112172
33. Tabassum T, Hasan M, Begum L (2018) Transient melting of an impure paraffin wax in a double-pipe heat exchanger: Effect of forced convective flow of the heat transfer fluid. S*ol Energy* 159: 197–211. https://doi.org/10.1016/j.solener.2017.10.082

34. Liu L, Zhang X, Xu X, et al. (2020) The research progress on phase change hysteresis affecting the thermal characteristics of PCMs: A review. *J Mol Liq* 317: 113760. https://doi.org/10.1016/j.molliq.2020.113760
35. Rahman RA, Lahuri AH, Ismail I (2023) Thermal stress influence on the long-term performance of fast-charging paraffin-based thermal storage. *TSEP* 37: 101546. https://doi.org/10.1016/j.tsep.2022.101546

AIMS Press